ESTIMATION OF INSTRUMENT SPECTRAL RESPONSE FUNCTIONS USING SPARSE REPRESENTATIONS IN A DICTIONARY

Jihanne El Haouari [1,2], Jean-Michel Gaucel[3], Christelle Pittet[4], Jean-Yves Tourneret[1,2] and Herwig Wendt[2]

[1] TéSA laboratory, Toulouse, France. jihanne.elhaouari@tesa.prd.fr
[2] IRIT-ENSEEIHT, CNRS, Univ. Toulouse, Toulouse, France. firstname.lastname@irit.fr
[3] Thales Alenia Space Cannes, France jean-michel.gaucel@thalesaleniaspace.com
[4] Centre National d'Etudes Spatiales, Centre Spatial de Toulouse, France christelle.pittet@cnes.fr

ABSTRACT

Understanding greenhouse gas fluxes at the Earth's surface is becoming crucial in the context of climate change. The aim of the CNES/UKSA MicroCarb mission is therefore to map, on a planetary scale, the sources and sinks of carbon, the main greenhouse gas in the atmosphere. To do this, a spectrometer will be sent in space to acquire spectra in 4 narrow bands around wavelengths associated with O_2 and CO_2. However, measurement errors can occur due to the instrument used, and induce errors in the resulting trace gas concentrations. It is therefore crucial to estimate the spectral response of the instrument as accurately as possible. This paper investigates a new estimation method for this spectral response that uses a sparse representation in a dictionary of appropriate basis functions. This sparse representation is performed using the LASSO and Orthogonal Matching Pursuit (OMP) algorithms. Simulations conducted on data mimicking observations resulting from the MicroCarb instrument allow the performance of this method to be appreciated.

Index Terms— MicroCarb Mission, Instrument Spectral Responses, Sparse Representations.

1. INTRODUCTION

Spectrometers are widely used in remote sensing missions to determine trace gas concentrations. However, the optical elements within these instruments can introduce spectral distortions leading to errors in the measurements. It is crucial to characterize the instrument model and thus the associated Instrument Spectral Response Functions (ISRFs) to obtain accurate gas concentrations. These ISRFs are wavelength dependent and may change in flight due to several reasons (mechanical movements during launch, orbit changes ...). The MicroCarb instrument is a high-resolution spectrometer developed by the French Space Agency (CNES) in collaboration with UKSA (United Kindom Space Agency) to be launched around 2025 to measure and monitor carbon dioxide (CO_2) at the Earth's surface. It aims to ensure the continuity of carbon measurement missions such as OCO-2 and GoSAT [1, 2], helping our understanding of global carbon dynamics and different sources and sinks of carbon [3]. The concentrations of O_2 and CO_2 are calculated from spectra captured in four spectral bands. The fourth band is also used to improve and validate space-based measurements of greenhouse gases [4].

The estimation of the ISRFs consists in using a measurement of a spectrally known scene and comparing it with a spectral model of the scene convolved with the ISRFs [5, 6]. Each measurement s_l at the wavelength λ_l can be written as a convolution between the spectrum s_{th} and the ISRF I_l centered at λ_l:

$$s(\lambda_l) = (s_{\text{th}} * I_l)(\lambda_l) = \int_{\lambda_{\min}}^{\lambda_{\max}} s_{\text{th}}(\lambda_l - u) I_l(u) du. \quad (1)$$

When the theoretical spectrum s_{th} is known, estimating the ISRFs I_l can be formulated as an inverse problem for each wavelength λ_l.

In the literature, parametric models for the ISRFs have been widely used to solve this inverse problem [7]. However, these models cannot represent accurately the variety of all ISRF shapes encountered in practice. The main contribution of this work is to study new ISRF estimation methods based on sparse representations of the ISRFs in a dictionary of basis functions and to analyze their performance with respect to the state-of-the-art. Note that to the best of the author's knowledge, sparse representations have never been considered for ISRF estimation. Our results indicate that the extra flexibility of these representations over parametric models is particularly beneficial in the context of ISRF estimation. The paper is organized as follows. Section 2 formulates the ISRF estimation problem as a set of inverse problems and recalls some parametric models used for ISRF estimation. Section 3 introduces the new estimation model based on sparse representations of the ISRFs. Section 4 provides extensive results and performance comparisons for multiple kinds of ISRFs resulting from different scenes.

2. ISRF APPROXIMATION PROBLEM

2.1. Problem formulation

The ISRF of a spectrometer varies for each central wavelength λ_l. For each of these wavelength λ_l, the spectrometer acquires one spectral measurement denoted as $s_l \in \mathbb{R}$. Since there is only one measurement per function I_l, the ISRF estimation problem is not identifiable. In order to bypass this identifiability problem, we propose to estimate each ISRF I_l by using a collection of N_{obs} neighboring spectral measurements, assuming that the ISRF does not vary significantly in a neighborhood of λ_l. After wavelength discretization, the following observation model is obtained:

$$\boldsymbol{s}_l = \boldsymbol{S}_{\text{th},l} \boldsymbol{I}_l + \boldsymbol{\epsilon}_l, \quad (2)$$

where $\boldsymbol{s}_l = \left[s\left(\lambda_{l-\frac{N_{\text{obs}}}{2}}\right), ..., s\left(\lambda_{l+\frac{N_{\text{obs}}}{2}}\right)\right]^T \in \mathbb{R}^{N_{\text{obs}}+1}$ is the measurement vector, $\boldsymbol{S}_{\text{th}} = \left[\boldsymbol{s}_{\text{th},l-\frac{N_{\text{obs}}}{2}}, ..., \boldsymbol{s}_{\text{th},l+\frac{N_{\text{obs}}}{2}}\right]^T \in \mathbb{R}^{(N_{\text{obs}}+1)\times(N+1)}$ is a matrix containing the theoretical spectra interpolated at the window wavelengths, $\boldsymbol{I}_l$ is the discretized ISRF for the

lth window defined as $\boldsymbol{I}_l = \left[I_l(-\frac{N}{2}\Delta), ..., I_l(\frac{N}{2}\Delta)\right]^T \in \mathbb{R}^{N+1}$ where Δ is the ISRF wavelength interval, and $\boldsymbol{\epsilon}_l$ is the noise vector.

2.2. Parametric models

This section briefly recalls some of the most widely used models for ISRF estimation. The Gaussian model [8] approximates the ISRF at wavelenghth λ_l as

$$\boldsymbol{I}_{l,\boldsymbol{\beta}_{\mathrm{G}}} = A_G \exp\left[-\frac{(\lambda_l - \boldsymbol{\Delta} - \mu_{\mathrm{G}}).^2}{2\sigma^2}\right], \tag{3}$$

where $\boldsymbol{\beta}_G = [A_{\mathrm{G}}, \mu_{\mathrm{G}}, \sigma]^T$ is the unknown vector to estimate, $\boldsymbol{\Delta} = [-\frac{N}{2}\Delta, ..., \frac{N}{2}\Delta]^T \in \mathbb{R}^{N+1}$ is a vector containing the wavelengths of the grid and $.^p$ is the element-wise power operator of order p.
A generalized Gaussian model using a different power parameter k, called "Super-Gauss", was developed in [7] to estimate ISRFs:

$$\boldsymbol{I}_{l,\boldsymbol{\beta}_{\mathrm{SG}}} = A_{\mathrm{SG}} \exp\left(-\left|\frac{\lambda_l - \boldsymbol{\Delta} - \mu_{\mathrm{SG}}}{w}\right|^{.k}\right), \tag{4}$$

where $\boldsymbol{\beta}_{\mathrm{SG}} = [A_{\mathrm{SG}}, \mu_{\mathrm{SG}}, w, k]^T$ is the unknown vector to estimate. The inverse problems associated with these two models can be solved using a nonlinear least squares method, which minimizes the cost function $R_l(\boldsymbol{\beta}) = ||\boldsymbol{s}_l - \boldsymbol{S}_{\mathrm{th},l}\boldsymbol{I}_{l,\boldsymbol{\beta}}||_2^2$ with respect to the vector $\boldsymbol{\beta} \in \{\boldsymbol{\beta}_{\mathrm{G}}, \boldsymbol{\beta}_{\mathrm{SG}}\}$.
However, these two parametric models are not always flexible enough to represent all the ISRF shapes accurately with a small number of parameters. Therefore, we propose to study a new estimation method based on a sparse representation of the ISRFs in a dictionary of appropriate basis functions, which is presented in the next section.

3. PROPOSED ISRF ESTIMATION METHOD

3.1. Sparse representation of ISRFs

Sparse representations consist in expressing the unknown quantity of interest as a linear combination of a small number of atoms corresponding to the columns of a matrix referred to as dictionary. In the context of ISRF estimation, we propose to decompose each ISRF in a dictionary $\boldsymbol{\Phi} \in \mathbb{R}^{(N+1)\times N_{\mathrm{D}}}$ as follows:

$$\boldsymbol{I}_l \approx \boldsymbol{I}_l^K = \boldsymbol{\Phi}\boldsymbol{\alpha} = \sum_{k=1}^{K} \boldsymbol{\Phi}_{\gamma_k}\alpha_k, \tag{5}$$

where $\boldsymbol{\Phi}_{\gamma_k}$ is the γ_kth selected atom, i.e., the kth column of the dictionary $\boldsymbol{\Phi}$, and α_k is a non zero entry from the sparse coefficient vector $\boldsymbol{\alpha} \in \mathbb{R}^{N_{\mathrm{D}}}$. The dictionary is built in order to provide an efficient representation of the vectors $\boldsymbol{I}_l$ [9]. In this paper, $\boldsymbol{\Phi}$ is constructed using the N_{D} singular vectors associated with the largest singular values of a matrix composed of examples of ISRFs.

3.2. Inverse problem

The measured spectrum $\boldsymbol{s}_l$ can be rewritten using the ISRF decomposition of $\boldsymbol{I}_l$ as

$$\boldsymbol{s}_l \approx \boldsymbol{S}_{\mathrm{th},l}\boldsymbol{I}_l \approx \boldsymbol{S}_{\mathrm{th},l}\boldsymbol{\Phi}\boldsymbol{\alpha} = \boldsymbol{\Psi}_l\boldsymbol{\alpha}. \tag{6}$$

Thus, $\boldsymbol{s}_l$ can be expressed using the known modified dictionary $\boldsymbol{\Psi}_l$. Once the coefficient vector $\boldsymbol{\alpha}$ has been estimated using the spectral measurements and (6), it can be used to approximate the ISRF by substituting it in (5). The estimation of $\boldsymbol{\alpha}$ is referred to as sparse coding and can be mathematically formulated in different ways [10]. One possibility is to introduce a regularization based on the l_0 pseudo-norm of $\boldsymbol{\alpha}$ yielding the following problem:

$$\arg\min_{\boldsymbol{\alpha}} L(\boldsymbol{\alpha}, \mu) = \arg\min_{\boldsymbol{\alpha}} ||\boldsymbol{s}_l - \boldsymbol{\Psi}_l\boldsymbol{\alpha}||_2^2 + \mu||\boldsymbol{\alpha}||_0, \tag{7}$$

where μ is an appropriate regularization parameter. The problem (7) is non-convex and NP-hard. Many approximations and heuristics have been proposed and studied to compute a suitable approximate solution. A classical solution is to work with a convex relaxation of the problem by replacing the pseudo-norm l_0 by the norm l_1, which is known as the LASSO problem [11]. Another method determines the solution using greedy algorithms such as the Orthogonal Matching Pursuit (OMP) [12, 13]. The OMP algorithm is iterative and determines at each step the atom of the dictionary that best approximates the remaining residual, i.e., the atom that minimizes the residual error between the spectral measurements and the sparse coding representation obtained at the current step.

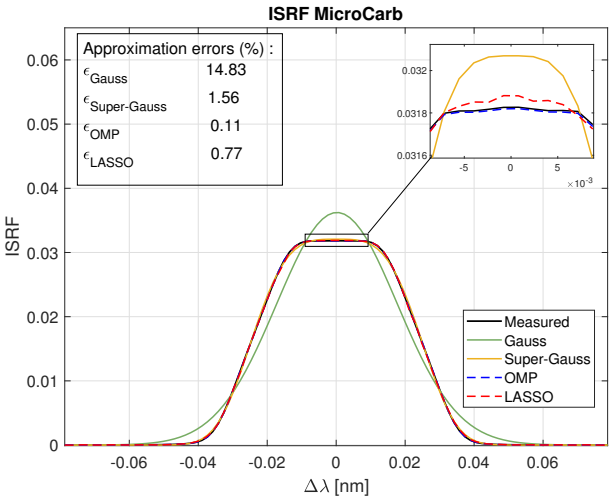

Fig. 1. Examples of ISRF estimates for one ISRF centered at around 1272.36 nm.

4. VALIDATION OF THE PROPOSED METHOD FOR THE MICROCARB SPECTROMETER

4.1. Data description

In order to analyze the potential interest of using sparse representations of ISRFs, this section compares the performance of the different methods (Gauss, Super-Gauss, OMP and LASSO) for ISRF estimation. The data used in this study was simulated by the CNES for the MicroCarb mission. For each band, the theoretical spectrum was obtained using the 4A/OP software [14] for the MicroCarb bands, and 1024 ISRFs and associated spectral measurements were generated. The parametric and sparse methods were applied to the B4 wavelength range ($1264.8 - 1282.3$ nm) corresponding to O_2. For all the results, the SNR level was set to 55 dB, which corresponds to the SNR level that is expected for the MicroCarb mission.

4.2. Experimental setup

The accuracy of the estimation methods is quantified by means of the reconstruction error for the measured spectra, and by the approx-

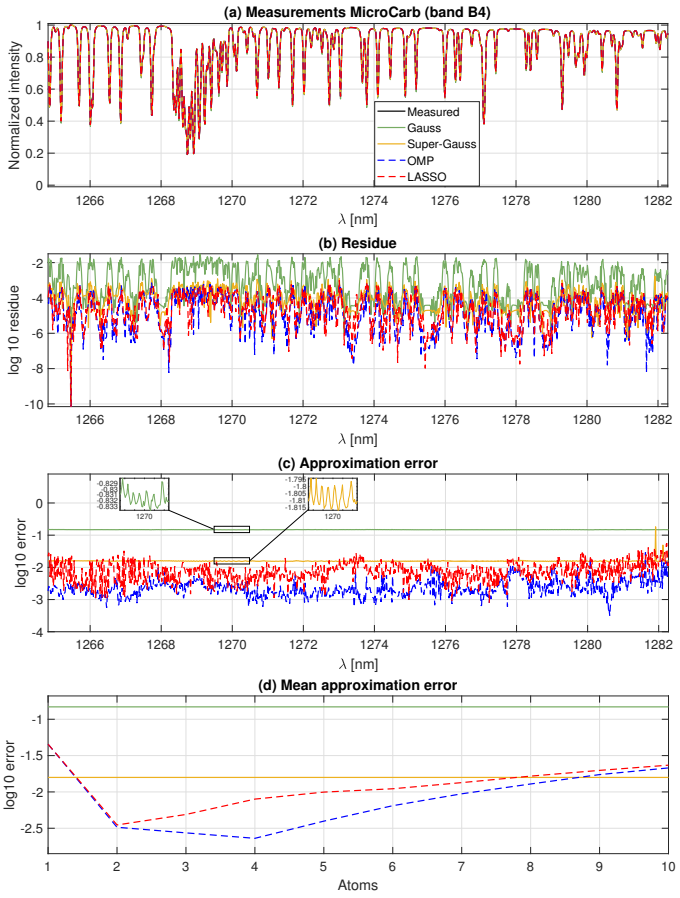

Fig. 2. Spectrum reconstruction (a), residual (b), ISRF approximation errors for all wavelengths (c) and mean errors for different numbers of selected atoms (d).

imation error for the ISRFs, defined for each wavelength as

$$\mathrm{E}_l = \sum_{n=1}^{N} |\boldsymbol{I}_l[n] - \hat{\boldsymbol{I}}_l[n]| / \sum_{n=1}^{N} \boldsymbol{I}_l[n].$$

In the MicroCarb mission, the ISRFs are considered to be well estimated when this error is below 1%. For the parametric models of Section 2.2, the parameters can be estimated using a non-linear least squares method, e.g., using the Nelder-Mead method [15] (MATLAB function *fminsearch*). For the sparse representations, we use our own implementation of the OMP algorithm and the MATLAB implementation of LASSO [16]. For LASSO, we re-estimate the value of the non-zero coefficients by using least squares in order to account for shrinkage biases [17]. The value of the parameter μ was set in order to reach the desired cardinality K. The size of the dictionary and the number of measurements in each window were set to $N_{\mathrm{D}} = 25$ and $N_{\mathrm{obs}} = 80$, which was found to yield the best results.

4.3. Performance comparison for different wavelengths

The dictionary was created using a singular value decomposition (SVD) of 103 out of 1024 examples of ISRFs in the B4 band. A typical example of such an ISRF is displayed in Fig. 1, as well as the corresponding approximation results obtained by the different methods, suggesting that the sparse methods provide more accurate results. The estimated ISRFs in the B4 band can be used in (2) to reconstruct the corresponding measured spectra. The reconstructed spectra and the residuals are shown in Fig. 2 for all methods (Gauss, Super-Gauss, OMP and LASSO).This figure also shows the ISRF approximation errors and the averaged ISRF reconstruction errors for different numbers of atoms. The results lead to the following conclusions:

First, the super-Gauss parameterization provides better ISRF approximations when compared to the Gaussian model, as claimed in [7]. However, the sparse methods manage to obtain even smaller errors and yield the expected precision less than 1%.

Second, the OMP algorithm yields better ISRF approximation results than LASSO. Indeed, the OMP solution yields globally the smallest spectral residuals, and in particular the smallest ISRF approximation errors, which are as small as 0.1% for certain wavelengths and 1 to 2 orders of magnitude smaller than those obtained with the super-Gaussian and Gaussian models, respectively.

Third, the averaged errors displayed in Fig. 2 (d) suggest that $K \in \{2, 3, 4\}$ atoms should be preferred for ISRF estimation. We recommend to use $K = 4$ atoms and the OMP algorithm for ISRF estimation, which yields globally the best results. The resulting ISRF estimation method is referred to as SPIRIT for "Sparse representation of Instrument spectral Responses usIng a dicTionary".

4.4. Performance comparison for different scenes

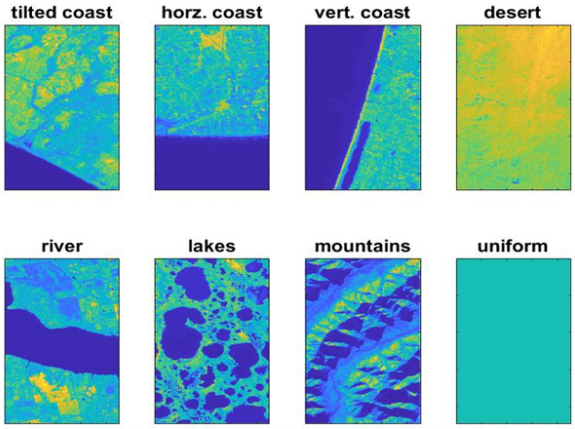

Fig. 3. Eight types of scenes associated with MicroCarb.

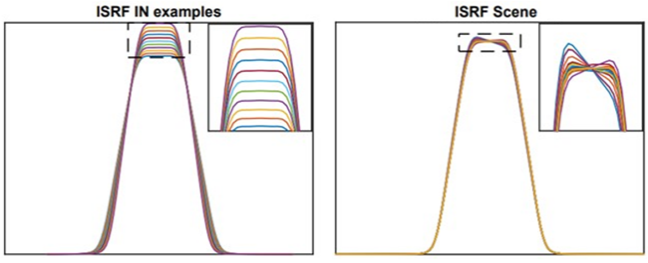

Fig. 4. ISRFs for a uniform scene with different central wavelengths (left) and different scenes for the same central wavelength (right).

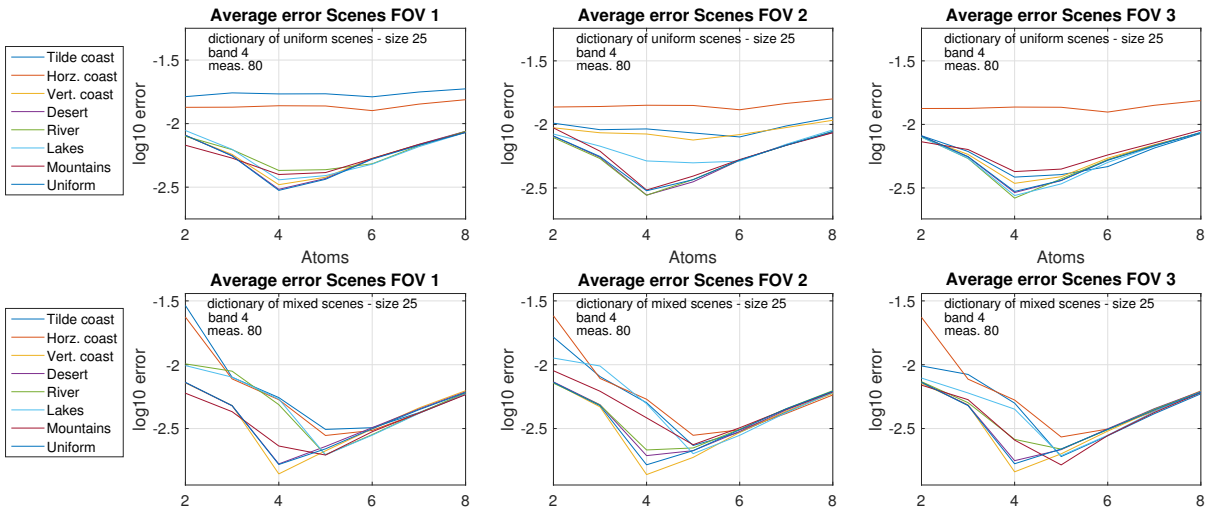

Fig. 5. Results obtained using OMP with uniform or mixed dictionary for different kind of ISRFs associated with different scenes and FOV.

In the MicroCarb mission, the shapes of the ISRFs are strongly dependent on the scene observed by the instrument and induce more variations than those observed for different consecutive wavelengths. Indeed, the MicroCarb instrument design makes the ISRF sensitive to the slit illumination during the integration time. Fig. 3 shows eight different scenes considered in this work with examples of ISRFs displayed in Fig. 4. Clearly, if the slit is not uniformly illuminated, the ISRF shape changes and can become asymmetric (e.g., for the horizontal coast profile, where the slit is blinded during one third of the integration time). This situation is more difficult to model than the case of ISRFs for a uniform scene studied in the previous section. This section evaluates the performance of SPIRIT to estimate a collection of ISRFs for different scenes and Fields Of View (FOV). Note that spectral measurements were simulated for a known theoretical spectrum as previously, here assuming that the ISRF for each scene and FOV has the same shape for all wavelengths, and the estimation error was estimated over wavelengths.

We first use the dictionary constructed from examples of ISRFs for uniform scenes. The results shown in Fig. 5 (left column) suggest that it can be difficult to estimate with high accuracy all the ISRFs for different scenes and FOV. This observation is illustrated in Fig. 6 for the estimation of the ISRF for the horizontal coast scene (a worst-case profile) using $K = 5$ atoms, calling for the use of a more diverse dictionary. To that end, we have built a new dictionary from a new matrix of ISRFs, comprising the previous 103 examples of ISRFs IN and in addition 3 ISRFs for non-uniform scenes (out of 24). The size of the dictionary remains fixed at $N_{\mathrm{D}} = 25$. The results are shown in Fig. 5 (right column) and indicate that with this slight modification, the use of this new and more diverse dictionary is effective: The SPIRIT method again achieves errors below the 1% criterion, sometimes approaching 0.1%. The lowest approximation errors are obtained depending on the scene with $K \in \{4, 5\}$ atoms, as in the previous experiment. Fig. 6 highlights the improvement made in ISRF estimation using a diversified dictionary, for an ISRF that was not included in its construction. Overall, these results suggests that SPIRIT is effective for the estimation of ISRFs of complicated shapes from a limited amount of spectral measurements, and provides very promising results with respect to the state-of-the-art.

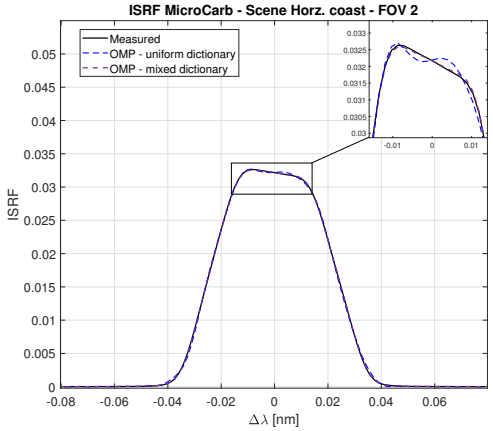

Fig. 6. ISRF estimates for the horizontal coast profile - FOV 2 using uniform or mixed dictionary (ISRF centered at $\lambda_l \approx 1272.36$ nm).

5. CONCLUSION

This paper proposes a new method for estimating the spectral response functions of spectrometers based on sparse representations in a dictionary of appropriate basis functions. The results obtained with data generated in agreement with the MicroCarb instrument suggest that the proposed method allows for a more flexible representation of spectral response functions and yields significantly smaller approximation errors than the parametric models used in the literature. The method seems to account for the variability of ISRF shapes and is operational for application to real-world data.

Future work will be devoted to the performance evaluation of the proposed method for estimating the spectral responses of other spectrometers described in the literature (such as GOME-2, OMI or OCO-2). In particular, it would be interesting to study the sensitivity of the proposed method to the choice of the dictionary. A more theoretical prospect consists of taking into account other physical effects that can modify the ISRF shapes. These effects such as scattered or stray light can degrade the estimation of spectral responses at some specific frequencies. Other spectrum errors due to radiometric defects or spectral shifts will also be considered.

6. REFERENCES

[1] A. Eldering et al., "The orbiting carbon observatory-2 early science investigations of regional carbon dioxide fluxes," *Science*, vol. 358, pp. eaam5745, 10 2017.

[2] R. Imasu et al., "Greenhouse gases observing satellite 2 (gosat-2): mission overview," *Prog. Earth Planet. Sci.*, vol. 10, pp. 33, 07 2023.

[3] E. Cansot, L. Pistre, M. Castelnau, P. Landiech, L. Georges, Y. Gaeremynck, and P. Bernard, "Microcarb instrument, overview and first results," *Proc. SPIE 12777, Inf. Conf. Space Optics*, vol. 12777, no. 1277734, pp. 1–13, 2022.

[4] J.-L. Bertaux, A. Hauchecorne, F. Lefèvre, F.-M. Bréon, L. Blanot, D. Jouglet, P. Lafrique, and P. Akaev, "The use of the 1.27μm o_2 absorption band for greenhouse gas monitoring from space and application to microcarb," *Atmospheric Measurement Techniques*, vol. 13, no. 6, pp. 3329–3374, 2020.

[5] M. Hamidouche and G. Lichtenberg, "In-flight retrieval of SCIAMACHY instrument spectral response function," *Remote Sens.*, vol. 10, no. 3, pp. 401, 2018.

[6] K. Sun, X. Liu, G. Huang, G. González Abad, Z. Cai, K. Chance, and K. Yang, "Deriving the slit functions from OMI solar observations and its implications for ozone-profile retrieval," *Atmos. Meas. Tech.*, vol. 10, no. 10, pp. 3677–3695, 2017.

[7] S. Beirle, J. Lampel, C. Lerot, H. Sihler, and T. Wagner, "Parameterizing the instrumental spectral response function and its changes by a super-Gaussian and its derivatives," *Atmos. Meas. Tech.*, vol. 10, no. 2, pp. 581–598, 2017.

[8] R. Munro, R. Lang, D. Klaes, G. Poli, C. Retscher, R. Lindstrot, R. Huckle, A. Lacan, M. Grzegorski, A. Holdak, A. Kokhanovsky, J. Livschitz, and M. Eisinger, "The GOME-2 instrument on the Metop series of satellites: instrument design, calibration, and level 1 data processing – an overview," *Atmos. Meas. Tech.*, vol. 9, no. 3, pp. 1279–1301, 2016.

[9] I. Tošić and P. Frossard, "Dictionary learning," *IEEE Signal Process. Mag.*, vol. 28, no. 2, pp. 27–38, 2011.

[10] Z. Zhang, Y. Xu, J. Yang, X. Li, and D. Zhang, "A survey of sparse representation: Algorithms and applications," *IEEE Access*, vol. 3, pp. 490–530, 2015.

[11] M. Tan, I. W. Tsang, and L. Wang, "Matching pursuit LASSO Part I: Sparse recovery over big dictionary," *IEEE Trans. Signal Process.*, vol. 63, no. 3, pp. 727–741, 2015.

[12] S. G. Mallat and Z. Zhang, "Matching pursuits with time-frequency dictionaries," *IEEE Trans. Signal Process.*, vol. 41, no. 12, pp. 3397–3415, 1993.

[13] Y. C. Pati, R. Rezaiifar, and P. S. Krishnaprasad, "Orthogonal matching pursuit: recursive function approximation with applications to wavelet decomposition," in *Proc. Asilomar Conf. Signals, Systems and Computers*, Pacific Grove, CA, USA, Nov. 1-3 1993, pp. 40–44.

[14] NOVELTIS, CNES, and LMD, "4A/OP - operational release for 4A - automatized atmospheric absorption atlas," https://4aop.noveltis.fr/references-and-publications.

[15] J. C. Lagarias, J. A. Reeds, M. H. Wright, and P. E. Wright, "Convergence properties of the Nelder-Mead simplex method in low dimensions," *SIAM J. Optim.*, vol. 9, pp. 112–147, 1998.

[16] R. Tibshirani, "Regression shrinkage and selection via the lasso," *Journal of the Royal Statistical Society (Series B)*, vol. 58, pp. 267–288, 1996.

[17] C.-H. Zhang and J. Huang, "The sparsity and bias of the Lasso selection in high-dimensional linear regression," *Ann. Stat.*, vol. 36, no. 4, pp. 1567 – 1594, 2008.